

Pressure-Driven Reversible Switching between *n*- and *p*-Type Conduction in Chalcopyrite CuFeS₂

HPSTAR
683-2019

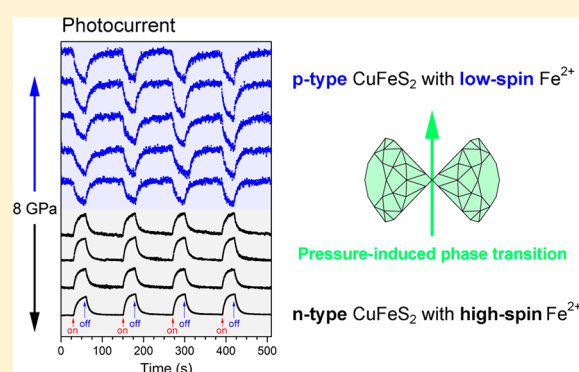
Ting Wen,[†] Yonggang Wang,^{*,†} Nana Li,[†] Qian Zhang,[†] Yongsheng Zhao,[†] Wenge Yang,^{*,†} Yusheng Zhao,^{*,‡} and Ho-kwang Mao[†]

[†]Center for High Pressure Science and Technology Advanced Research (HPSTAR), Beijing 100094, China

[‡]Department of Physics and Academy for Advanced Interdisciplinary Studies, Southern University of Science and Technology, Shenzhen 518055, China

Supporting Information

ABSTRACT: Temperature-dependent switching between *p*- and *n*-type conduction is a newly observed phenomenon in very few Ag-based semiconductors, which may promote fascinating applications in modern electronics. Pressure, as an efficient external stimulus that has driven collective phenomena such as spin-crossover and Mott transition, is also expected to initialize a conduction-type switching in transition metal-based semiconductors. Herein, we report the observation of a pressure-driven dramatic switching between *p*- and *n*-type conduction in chalcopyrite CuFeS₂, associated with a structural phase transition. Under compression around 8 GPa, CuFeS₂ undergoes a phase transition with symmetry breakdown from space group *I*-42*d* to space group *I*-4 accompanying with a remarkable volume shrinkage of the FeS₄ tetrahedra. A high-to-low spin-crossover of Fe²⁺ (*S* = 2 to *S* = 0) is manifested along with this phase transition. Instead of pressure-driven metallization, a surprising semiconductor-to-semiconductor transition is observed associated with the structural and electronic transformations. Significantly, both photocurrent and Hall coefficient measurements confirm that CuFeS₂ undergoes a reversible pressure-driven *p*–*n* conduction type switching accompanying with the structural phase transition. The absence of cationic charge transfer between copper and iron during the phase transition is confirmed by both X-ray absorption near-edge spectra (Cu/Fe, K-edge) and total-fluorescence-yield X-ray absorption spectra (Fe, K-edge) results, and the valence distribution maintains Cu²⁺Fe²⁺S₂ in the high-pressure phase. The observation of an abrupt pressure-driven *p*–*n* conduction type switching in a transition metal-based semiconductor paves the way to novel pressure-responsive switching devices.



INTRODUCTION

Materials with phase change or physical property change abilities are some of the most promising candidates for switch or memory applications.^{1,2} A case in point is the Ge–Sb–Te phase change alloys, which are already widely employed in rewriteable optical storage products such as compact disks (CD), digital versatile disks (DVD), and Blu-ray disks for nonvolatile electronic memory.^{3,4} These materials crucially exhibit dramatic optical and electric changes between the two states and also several other physical/chemical properties such as high phase transition speed and good chemical stability for industrial applications.² Recently, an emerging class of inorganic semiconductors with fascinating switching ability between *p*- and *n*-type conduction upon temperature change has been discovered, which shows great potential in transistor or memory applications.⁵ To date, such temperature-dependent *p*–*n* switching materials are limited in only a few Ag-based compounds: AgCuS,⁶ AgBiSe₂,⁷ Ag₁₀Te₄Br₃,⁸ and their derivatives.^{9,10} All of them show dramatic and reversible *p*–*n*-type conduction switching upon heating as evidenced by the

Seebeck coefficient analyses. Although temperature-dependent *p*–*n* switching always occurs accompanying with structural phase transitions in the above-mentioned materials, the underlying mechanism unfortunately is not clear yet and there is no guidance for future exploration of *p*–*n* switching semiconductors.

Pressure, as an alternative external stimulus as temperature, has been manifested to be an efficient tool to modify the structure and physical properties of functional materials in the past two decades.¹¹ From the situation that collective pressure-driven switching between bistable states such as spin-crossover,^{12–15} piezochromism,^{16,17} and insulator-to-metal transition have been realized similar as those upon temperature variation, pressure-driven *p*–*n* switching should not be an exception. Actually, pressure-induced *p*–*n* switching has been observed in several distinct systems including elements (Si, Ge, Sn, Sc, Mn),^{18–20} metal chalcogenides (Bi₂Te₃, ZrTe₃),^{21,22}

Received: October 18, 2018

Published: November 28, 2018

and transition metal oxides (Ti_2O_3 , Mn_2O_3).^{23,24} In situ thermoelectric power measurement results show that all of these materials undergo a gradual conduction-type reversal on the scale of several to tens of GPa. Innovative applications of pressure-driven p - n switching materials are suggested such as the fabrication of single-component n - p or n - p - n junctions by applied stress. However, if compared with the temperature-dependent counterparts,⁵ the pressure-driven p - n switching materials are still far away from meeting the requirements of practical applications. A reversible and abrupt conduction-type change within a narrow pressure interval is required.²

Inspired by the temperature-driven switching between p - and n -type conduction in AgCuS , AgBiSe_2 , and $\text{Ag}_{10}\text{Te}_4\text{Br}_3$, a possible route to an abrupt conduction-type crossover is to introduce an incidental structural transformation.⁶⁻⁸ In other words, a dramatic p - n switching should occur as a result of the intrinsic property change between the low-pressure and the high-pressure phases rather than the stress effect only. In this article, we report the progress of our pursuit of pressure-driven p - n switching materials in pressure-driven spin-crossover systems. Through comprehensive in situ characterization under high pressure, we demonstrate that the chalcopyrite CuFeS_2 is a novel p - n switching material under high pressure. The conduction behavior of CuFeS_2 is studied associated with the crystal structure evolution, the spin-crossover of iron, the semiconductor-to-semiconductor transition, and a possible intermetallic charge transfer process.

EXPERIMENTAL DETAILS

Characterization of Pristine Materials. High-quality CuFeS_2 single crystals were obtained from a natural core in Jiangxi Province, China. The composition analysis was performed by energy-dispersive spectra (EDS) using a Quanta 250 FEG FEI Scanning Electron Microscope (SEM). The phase purity was confirmed by X-ray diffraction (XRD) at room temperature and ambient pressure using a Bruker D8 Advance diffractometer with a $\text{Cu K}\alpha$ source.

In Situ High-Pressure Characterization. A symmetrical diamond anvil cell (DAC) was used to generate high pressure up to 40 GPa. Rhenium gaskets were preindented to 40–50 μm in thickness, and holes of about 150 μm diameter were laser drilled to serve as the sample chambers. For the in situ powder XRD measurements, a well-grinded and precompressed CuFeS_2 pallet was loaded in the chamber and silicone oil was used as the pressure transmitting medium (PTM). The pressures were determined by the ruby fluorescence method.²⁵ The XRD patterns were collected at beamline 16 BM-D at the Advanced Photon Source (APS), Argonne National Laboratory (ANL), and the 4W2 High Pressure Station in the Beijing Synchrotron Radiation Facility (BSRF). Focused monochromatic X-ray beams with about 20 μm in diameter and wavelengths of 0.3066 and 0.6199 \AA were used for the diffraction experiments at the APS and BSRF, respectively. The diffraction data were recorded by a MAR345 image plate at the APS and a Pilatus detector at the BSRF. High-purity CeO_2 powder was used as the standard for calibration.

The high-pressure X-ray emission spectra (XES) and total-fluorescence-yield X-ray absorption spectra (TFY-XAS) experiments on the Fe K-edge were conducted at beamline 16 ID-D at the APS. In these measurements, Be gaskets were used and silicone oil served as PTM. X-ray absorption near-edge spectra (XANES) at both the Fe and the Cu K-edge were collected at beamline 20 ID-C, APS, ANL. No PTM was used to ensure the uniform thickness, and nanodiamond anvils were used to avoid the diamond diffraction glitches.

In situ high-pressure resistance measurements were performed using the four-point-probe method with a 2182A nanovoltmeter, a Keithley 6221 current source, and a 7001 switch system. The Hall coefficient was measured using a Physical Property Measurement

System (PPMS, Quantum Design). In situ high-pressure photocurrent measurements were performed using a Zennium electrochemical workstation (Zahner) and a 50 W Xe lamp as the light source.²⁶

The total energy calculations were performed using the projector augmented wave method (PAW) as implemented in Vienna ab initio Simulation Package (VASP).²⁷ The Perdew–Burke–Ernzerhof (PBE) was treated as the exchange–correlation potential within the generalized gradient approximation (GGA).²⁸ The structure models are described in the following text.

Data Analyses. The powder XRD patterns were integrated with the Dioptas program.²⁹ Lattice parameter refinements were performed by using the FULLPROF program.³⁰ The quantitative analyses of the XES data were conducted following the IAD method.³¹

RESULTS AND DISCUSSION

Chalcopyrite (CuFeS_2) is a common mineral representing most of the world supplies of copper. From the viewpoint of structural chemistry, CuFeS_2 adopts a tetragonal zincblende-type structure with FeS_4 and CuS_4 tetrahedra connecting in a corner-sharing manner. CuFeS_2 is an antiferromagnetic semiconductor. Different from its simple appearance, CuFeS_2 indeed exhibits unusual electrical and magnetic properties, which are still not well understood yet. Even more surprisingly, there are debates on the valences of iron and copper in CuFeS_2 at ambient conditions because of the incongruous results from different techniques such as magnetic susceptibility, neutron scattering, Mössbauer spectroscopy, and XANES.³²⁻³⁶ Under high pressure, the structural and property behaviors of CuFeS_2 are also controversial. Pitt et al.³⁷ reported two phase transitions at 2.8 and 7 GPa respectively, the latter of which was assigned transforming to the NaCl-type structure accompanying with a semiconductor-to-metal transition. However, subsequent studies only observed the second phase transition around 7 GPa.^{38,39} Kobayashi et al. believed that it was a pressure-induced amorphization rather than phase transition.⁴⁰ In this work, we only report our experimental results and do not wish to unify all of the disputes.

Pressure-Induced Phase Transition. High-quality single crystals with elemental proportion of $\text{CuFe}_{0.99}\text{S}_2$ were used for all of the studies in this work (Figure S1). Ambient CuFeS_2 crystallizes in a tetragonal structure with space group $I-42d$. Under compression, a phase transition occurs evidently around 8 GPa (Figure S2). After careful analyses, we prefer to choose the tetragonal space group $I-4$ for the high-pressure phase rather than the previously proposed NaCl-type ($P4/mmm$) or β -Sn-type structure ($P-4m2$).^{37,38} Figure 1 shows the lattice

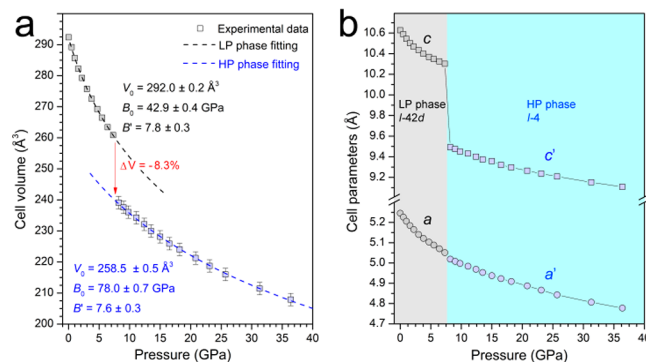


Figure 1. (a) Cell volumes as a function of applied pressure for the low-pressure (LP) and high-pressure (HP) phases of CuFeS_2 . (b) Cell parameters of CuFeS_2 as a function of applied pressure.

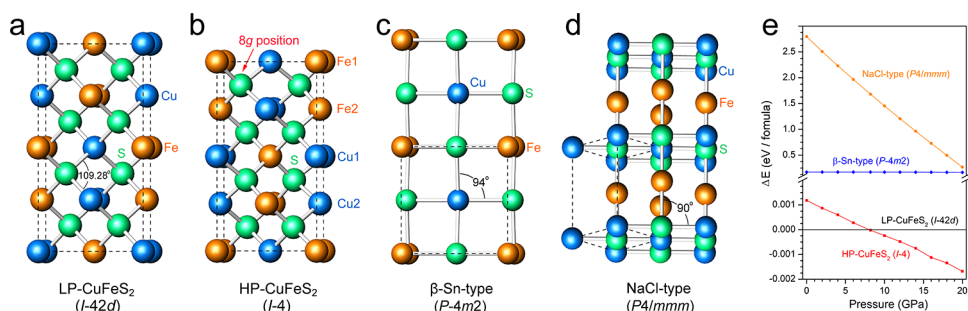


Figure 2. Crystal structures for (a) the ambient phase of CuFeS_2 with space group $I-42d$, (b) the proposed high-pressure phase of CuFeS_2 with space group $I-4$, (c) the β -Sn-type structure with space group $P-4m2$, and (d) the NaCl-type structure with space group $P4/mmm$. (e) Total energy diagram for the proposed high-pressure polymorphs of CuFeS_2 as a function of applied pressure with the ambient $I-42d$ structure as a reference.

volume and cell parameter evolutions of CuFeS_2 as a function of pressure. The phase transition around 8 GPa occurs accompanying with a volume collapse of about 8.3%, which is very possible due to the spin-crossover of transition metal ions. The low-pressure phase of CuFeS_2 is relatively soft ($B_0 = 42.9$ GPa), and the high-pressure phase is a little harder ($B_0 = 78.0$ GPa). The large volume collapse is mainly from the shrinkage along the c axis, indicating abruptly shortened Fe–Fe and Cu–Cu distances across the phase transition. CuFeS_2 returns to the original structure after pressure release (Figure S3).

Figure 2 shows the structure of CuFeS_2 at ambient pressure and possible structures at high-pressure conditions. The structure model with space group $I-4$ is more reasonable than the previously proposed NaCl- and β -Sn-type models^{37,38} due to the following reasons: (1) $I-4$ is the maximal nonisomorphic subgroup of $I-42d$; (2) the coordinates of the 8g position in the $I-4$ model is totally released to (x, y, z) to allow the shrinkage of the FeS_4 tetrahedra alone, which corresponds well to the pressure-induced spin-crossover of Fe^{2+} ; (3) the coordination manner and bond angles are unreliable and far from a regular tetrahedron ($109^\circ 28'$); (4) the $I-4$ model fits the experimental XRD patterns well (Figure S4), while the other two do not. Table 1 provides the refined

Table 1. Crystal Data and Fractional Atomic Coordinates of the Ambient and High-Pressure Phases of CuFeS_2 at 8.2 GPa

0 GPa, space group $I-42d$, $a = 5.246(3)$ Å, $c = 10.626(6)$ Å				
atoms	Wyckoff	x	y	z
Cu	4a	0	0	0
Fe	4b	0	0	0.5
S	8d	0	0	0.5
8.2 GPa, space group $I-4$, $a = 5.019(6)$ Å, $c = 9.493(8)$ Å				
atoms	Wyckoff	x	y	z
Fe1	2a	0	0	0
Cu1	2b	0	0	0.5
Fe2	2c	0	0.5	0.25
Cu2	2d	0	0.5	0.75
S	8g	0.2225	0.2496	0.1255

crystal data and atomic positions of the ambient and high-pressure phases of CuFeS_2 at 8.2 GPa, respectively. The serious broadening of the XRD patterns of the high-pressure phase can also be explained by the not-well-fixed 8g position in the $I-4$ structure under inhomogeneous pressure effect. Moreover, total energy calculations based on these structure models also

support the choice of $I-4$ structure since it has the lowest formation energy above 8 GPa (Figure 2e).

Pressure-Driven Spin-Crossover of Fe^{2+} and the Semiconductor-to-Semiconductor Transition. The large volume collapse of about 8.3% during the phase transition of CuFeS_2 is expected to be associated with pressure-driven spin-crossover of Fe^{2+} . Figure 3 presents the Fe K_β XES spectra of

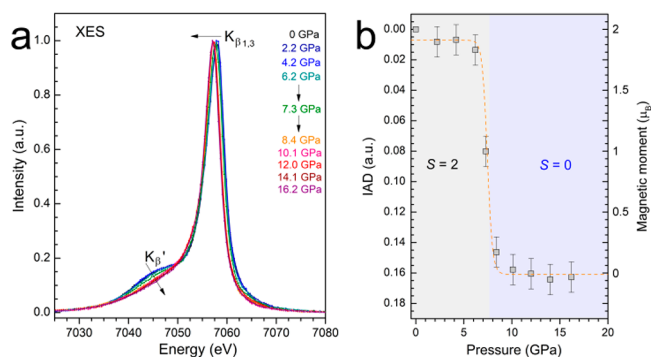


Figure 3. Fe spin states probed with in situ high-pressure XES method. (a) Fe K_β XES of CuFeS_2 as a function of applied pressures. (b) IAD values at high pressure obtained relative to the ambient spectra of CuFeS_2 . Dashed line is drawn as a guide to the eye and not a fit to the data.

CuFeS_2 under compression up to 16.2 GPa. Since K_β emissions are determined by the state interactions between the 3p core hole and the partially filled 3d shell electrons, one can distinguish the high-to-low-spin transition qualitatively from the vanishing of the satellite K_β' peak and the position of $K_{\beta 1,3}$.⁴¹ Below 7.3 GPa, well-defined K_β' peaks are observed for CuFeS_2 , indicating a high-spin state of Fe^{2+} with $S = 2$. The K_β' peak decreases abruptly with increasing pressure beyond 7.3 GPa, and the $K_{\beta 1,3}$ peak shifts to lower energy correspondingly. This evidence indicates the occurrence of pressure-driven spin-crossover of Fe^{2+} along with the structural phase transition. Quantitative analysis results using the IAD method³¹ are shown in Figure 3b. The IAD value changes from the high-spin level of $S = 2$ to the low-spin level of $S = 0$ is evidenced around 7 GPa, indicating a complete collapse of the Fe^{2+} moments in CuFeS_2 . According to crystal-field theory, a pressure-induced spin-crossover is governed by the magnitude of the crystal-field splitting energy ($\Delta = 10Dq$) and the Hund's intra-atomic exchange energy (J). Thus, the XES results point to the collapse of the FeS_4 tetrahedra during the pressure-induced phase transition, which also supports the choice of the $I-4$ structure model.

Figure 4 shows the electric resistance of CuFeS₂ as a function of pressure and temperature. Along with the pressure

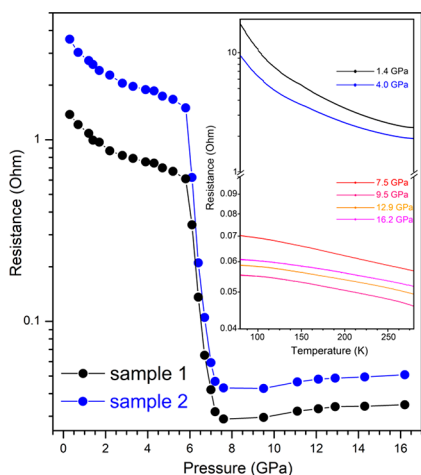


Figure 4. Electric resistances of CuFeS₂ as a function of pressure. (Inset) Temperature dependence of the resistance of CuFeS₂ under compression. Near 7 GPa, the electric resistance drops sharply with about 2 orders of magnitude at room temperature while the R - T curves confirm the remaining semiconductor behavior up to 16.2 GPa.

increases to approximately 7 GPa, the resistance curves drop quickly by about 2 orders of magnitude, indicating an electronic configuration transformation along with the pressure-induced structural phase transition. The tendencies of the R - T plots indicate a semiconductor-to-semiconductor transition along with the resistance dropping. In most cases, transition metal chalcogenides undergo a semiconductor-to-metal transition upon compression, especially when structural phase transition and spin-crossover of the transition metal ions occur at the same time. A surprising pressure-driven electronic configuration reconstruction provides an unprecedented opportunity for realizing controllable switch in a single-component semiconductor.

Pressure-Driven p - n Conduction Switching. One of the most important purposes of this work is pursuing dramatic pressure-driven p - n switching phenomenon. Besides the thermoelectric power (Seebeck coefficient) measurement, the photocurrent and Hall coefficient are also direct characterization methods to detect the carrier type and concentration of a semiconductor under high pressure.^{26,42} The setup within the DAC is the same as that described previously.²⁶ Figure 5a displays the photocurrent measurement results of CuFeS₂ as a function of pressure. The response to white light irradiation

(Xe lamp) is evident along with light on and off, and the reversal of the photocurrent direction indicates an n -type to p -type conduction transition. Quantitative analysis result shows a dramatic n - p switching around 8 GPa (Figure 5b). The photocurrent reversal is manifested reversible with a hysteresis of about 3 GPa, consistent with the structure analysis results. The pressure-driven switching between n - and p -type conduction of CuFeS₂ is also confirmed by in situ Hall coefficient measurements (Figure 5c and 5d). A tendency overturn of the Hall resistance occurs around 9 GPa, and the derived Hall coefficient shows a similar profile with those from the photocurrent measurements. There is an abrupt jump of the Hall coefficient by 1 order of magnitude at 5.0 GPa, which is often observed in the temperature-dependent p - n switching, but we are not sure if it is an intrinsic behavior of CuFeS₂ under high pressure. Moreover, the little divergence of the transition pressure (7–9 GPa) can be attributed to the different sample conditions for pressure calibration, e.g., with or without PTM.

Absence of Charge Transfer between Cu²⁺ and Fe²⁺.

Pressure-induced cationic valence exchange between Cu and Fe has been observed in delafossite CuFeO₂.⁴³ In the case of CuFeS₂, it is highly expected that the pressure-driven structure transition, spin-crossover, and p - n switching are associated with a cationic charge transfer. Figure 6 displays the XAENS and TFY-XAS results of CuFeS₂ under high pressure. As we known, a XAS profile can reflect both the chemical environment and the valence of a specific element in a given structure, and the latter is characteristically determined by the position of the absorption edge. First, we demonstrate that the valence of Cu and Fe at ambient conditions is Cu²⁺Fe²⁺S₂ in our sample, compared to Fe, FeS, and Fe₂O₃ standards from both the XAENS and the TFY-XAS signals. Then, despite the changes of both profiles around the K-edge of Cu and Fe before and after the phase transition (especially for the white lines), no evident shift of the K-edge is observed for both Cu and Fe. Thus, we conclude that there is no cationic charge transfer along with the phase transition around 8 GPa in our CuFeS₂ sample. Fourier-transformed profiles for the coordination environments of Fe and Cu confirm the simultaneous shrinkage of the FeS₄ tetrahedra and a slight expansion of the CuS₄ tetrahedra (Figure 6c and 6d). The different charge distribution and valence-change behavior of CuFeO₂ and CuFeS₂ under both ambient and high-pressure conditions may be attributed to the relative electronegativity of the ligands and also the formation history of the materials.

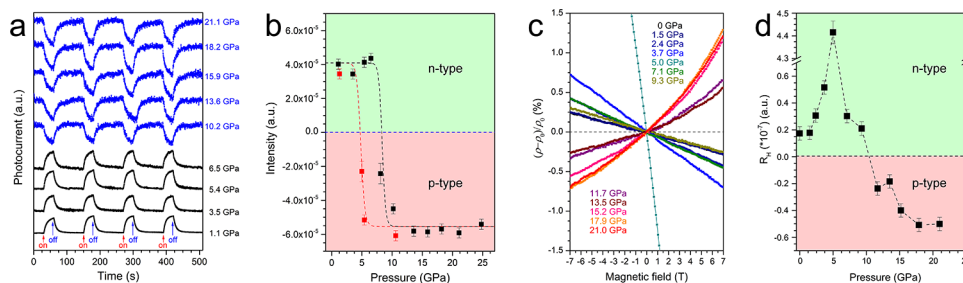


Figure 5. (a) Photocurrent, (b) photocurrent amplitude and direction, (c) normalized Hall resistance, and (d) derived Hall coefficient of CuFeS₂ as a function of pressure. Dashed lines in panels b and d are drawn as a guide to the eye and not a fit to the data.

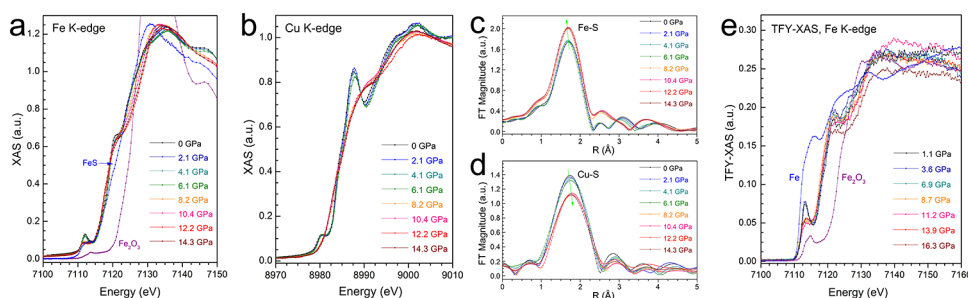


Figure 6. (a, b) XANES on the K-edges of both Fe and Cu for CuFeS₂ as a function of pressure. (c, d) Fourier-transformed profiles for the coordination environments of Fe and Cu in CuFeS₂ as a function of pressure. (e) TFY-XAS on the Fe K-edge for CuFeS₂ as a function of pressure. Fe metal, FeS, and Fe₂O₃ are used as references for Feⁿ⁺ with $n = 0, 2$ and 3 , respectively.

CONCLUSION

In summary, we report a pressure-driven reversible switching between p - and n -type conduction in CuFeS₂ associated with a dramatic structural phase transition and a spin-crossover of Fe²⁺. Symmetry breakdown from space group $I-42d$ to $I-4$ occurs along with the phase transition, and remarkable volume shrinkage of the FeS₄ tetrahedra is observed. Electric transport measurements confirm a semiconductor-to-semiconductor transition instead of a pressure-driven metallization for traditional semiconductors. The pressure-driven p - n type conduction switching is evidenced in both photocurrent and Hall coefficient measurements. We also confirm the absence of cationic valence exchange between copper and iron during the phase transition by XANES on both the K-edges of Cu and Fe and TFY-XAS on the Fe K-edge. We believe the discovery of the abrupt pressure-driven switching between p - and n -type conduction in magnetic semiconductors open a new door to pressure-responsive switching materials.

ASSOCIATED CONTENT

Supporting Information

The Supporting Information is available free of charge on the ACS Publications website at DOI: 10.1021/jacs.8b11269.

EDS analysis results and in situ high-pressure XRD patterns of CuFeS₂; XRD patterns of the recovered sample; selective refinement results and bond length changes of CuFeS₂ (PDF)

AUTHOR INFORMATION

Corresponding Authors

*yonggang.wang@hpstar.ac.cn

*yangwg@hpstar.ac.cn

*zhaoy@sustc.edu.cn

ORCID

Yonggang Wang: 0000-0003-4816-9182

Wenge Yang: 0000-0002-1825-2826

Notes

The authors declare no competing financial interest.

ACKNOWLEDGMENTS

This work was supported by the National Key R&D Program of China (2018YFA0305900) and National Natural Science Foundation of China (51527801 and U1530402). HPCAT operations are supported by DOE-NNSA under Award No. DE-NA0001974 with partial instrumentation funding by NSF. APS is supported by DOE-BES, under contract No. DE-AC02-06CH11357. W.Y. acknowledges Prof. T. Irifune for providing

a pair of nanodiamonds for the high-pressure XAS measurements.

REFERENCES

- Wuttig, M. Phase-change materials: Towards a universal memory? *Nat. Mater.* **2005**, *4*, 265–266.
- Wuttig, M.; Yamada, N. Phase-change materials for rewritable data storage. *Nat. Mater.* **2007**, *6*, 824–832.
- Yamada, N.; Ohno, E.; Akahira, N.; Nishiuchi, K.; Nagata, K.; Takao, M. High speed overwriteable phase change optical disk material. *Jpn. J. Appl. Phys.* **1987**, *26*, 61–66.
- Yamada, N.; Ohno, E.; Nishiuchi, K.; Akahira, N.; Takao, M. Rapid phase transitions of GeTe-Sb₂Te₃ pseudobinary amorphous thin films for an optical disk memory. *J. Appl. Phys.* **1991**, *69*, 2849–2856.
- Guin, S. N.; Biswas, K. Temperature driven p - n - p type conduction switching materials: current trends and future directions. *Phys. Chem. Chem. Phys.* **2015**, *17*, 10316–10325.
- Guin, S. N.; Pan, J.; Bhowmik, A.; Sanyal, D.; Waghmare, U. V.; Biswas, K. Temperature dependent reversible p - n - p type conduction switching with colossal change in thermopower of semiconducting AgCuS. *J. Am. Chem. Soc.* **2014**, *136*, 12712–12720.
- Xiao, C.; Qin, X.; Zhang, J.; An, R.; Xu, J.; Li, K.; Cao, B.; Yang, J.; Ye, B.; Xie, Y. High thermoelectric and reversible p - n - p conduction type switching integrated in dimetal chalcogenide. *J. Am. Chem. Soc.* **2012**, *134*, 18460–18466.
- Nilges, T.; Lange, S.; Bawohl, M.; Deckwart, J. M.; Janssen, M.; Wiemhöfer, H.-D.; Decourt, R.; Chevalier, B.; Vannahme, J.; Eckert, H.; Wehlich, R. Reversible switching between p - and n -type conduction in the semiconductor Ag₁₀Te₄Br₃. *Nat. Mater.* **2009**, *8*, 101–108.
- Dutta, M.; Sanyal, D.; Biswas, K. Tuning of p - n - p -type conduction in AgCuS through cation vacancy: Thermopower and positron annihilation spectroscopy investigations. *Inorg. Chem.* **2018**, *57*, 7481–7489.
- Roy, P.; Waghmare, V.; Tanwar, K.; Maiti, T. Large change in thermopower with temperature driven p - n type conduction switching in environment friendly Ba_xSr_{2-x}Ti_{0.8}Fe_{0.8}Nb_{0.4}O₆ double perovskites. *Phys. Chem. Chem. Phys.* **2017**, *19*, 5818–5829.
- Mao, H.-K.; Chen, X.-J.; Ding, Y.; Li, B.; Wang, L. Solids, liquids, and gases under high pressure. *Rev. Mod. Phys.* **2018**, *90*, 015007.
- Pinkowicz, D.; Rams, M.; Mišek, M.; Kamenev, K. V.; Tomkowiak, H.; Katrusiak, A.; Sieklucka, B. Enforcing multifunctionality: a pressure-induced spin-crossover photomagnet. *J. Am. Chem. Soc.* **2015**, *137*, 8795–8802.
- Wang, Y.; Bai, L.; Wen, T.; Yang, L.; Gou, H.; Xiao, Y.; Chow, P.; Pravica, M.; Yang, W.; Zhao, Y. Giant pressure-driven lattice collapse coupled with intermetallic bonding and spin-state transition in manganese chalcogenides. *Angew. Chem., Int. Ed.* **2016**, *55*, 10350–10353.
- Wang, Y.; Zhou, Z.; Wen, T.; Zhou, Y.; Li, N.; Han, F.; Xiao, Y.; Chow, P.; Sun, J.; Pravica, M.; Cornelius, A. L.; Yang, W.; Zhao, Y.

Pressure-driven cooperative spin-crossover, large-volume collapse, and semiconductor-to-metal transition in manganese(II) honeycomb lattices. *J. Am. Chem. Soc.* **2016**, *138*, 15751–15757.

(15) Wang, Y.; Ying, J.; Zhou, Z.; Sun, J.; Wen, T.; Zhou, Y.; Li, N.; Zhang, Q.; Han, F.; Xiao, Y.; Chow, P.; Yang, W.; Struzhkin, V. V.; Zhao, Y. Emergent superconductivity in an iron-based honeycomb lattice initiated by pressure-driven spin-crossover. *Nat. Commun.* **2018**, *9*, 1914.

(16) Jaffe, A.; Lin, Y.; Mao, W. L.; Karunadasa, H. I. Pressure-induced conductivity and yellow-to-black piezochromism in a layered Cu-Cl hybrid perovskite. *J. Am. Chem. Soc.* **2015**, *137*, 1673–1678.

(17) Umeyama, D.; Lin, Y.; Karunadasa, H. I. Red-to-black piezochromism in a compressible Pb-I-SCN layered perovskite. *Chem. Mater.* **2016**, *28*, 3241–3244.

(18) Ovsyannikov, S. V.; Korobeinikov, I. V.; Morozova, N. V.; Misiuk, A.; Abrosimov, N. V.; Shchennikov, V. V. Smart[®] silicon: Switching between *p*- and *n*-conduction under compression. *Appl. Phys. Lett.* **2012**, *101*, 062107.

(19) Korobeinikov, I. V.; Morozova, N. V.; Shchennikov, V. V.; Ovsyannikov, S. V. Dramatic changes in thermoelectric power of germanium under pressure: Printing *n-p* junctions by applied stress. *Sci. Rep.* **2017**, *7*, 44220.

(20) Morozova, N. V.; Shchennikov, V. V.; Ovsyannikov, S. V. Features and regularities in behavior of thermoelectric properties of rare-earth, transition, and other metals under high pressure up to 20 GPa. *J. Appl. Phys.* **2015**, *118*, 225901.

(21) Ovsyannikov, S. V.; Morozova, N. V.; Korobeinikov, I. V.; Lukyanova, L. N.; Manakov, A. Y.; Likhacheva, A. Y.; Ancharov, A. I.; Vokhmyanin, A. P.; Berger, I. F.; Usov, O. A.; Kutasov, V. A.; Kulbachinskii, V. A.; Okada, T.; Shchennikov, V. V. Enhanced power factor and high-pressure effects in (Bi,Sb)₂(Te,Se)₃ thermoelectrics. *Appl. Phys. Lett.* **2015**, *106*, 143901.

(22) Morozova, N. V.; Korobeinikov, I. V.; Kurochka, K. V.; Titov, A. N.; Ovsyannikov, S. V. Thermoelectric properties of compressed titanium and zirconium trichalcogenides. *J. Phys. Chem. C* **2018**, *122*, 14362–14372.

(23) Ovsyannikov, S. V.; Wu, X.; Garbarino, G.; Núñez-Regueiro, M.; Shchennikov, V. V.; Khmeleva, J. A.; Karkin, A. E.; Dubrovinskaia, N.; Dubrovinsky, L. High-pressure behavior of structural, optical, and electronic transport properties of the golden Th₂S₃-type Ti₂O₃. *Phys. Rev. B: Condens. Matter Mater. Phys.* **2013**, *88*, 184106.

(24) Ovsyannikov, S. V.; Karkin, A. E.; Morozova, N. V.; Shchennikov, V. V.; Bykova, E.; Abakumov, A. M.; Tsirlin, A. A.; Glazyrin, K. V.; Dubrovinsky, L. A hard oxide semiconductor with a direct and narrow bandgap and switchable *p-n* electrical conduction. *Adv. Mater.* **2014**, *26*, 8185–8191.

(25) Mao, H. K.; Xu, J.; Bell, P. M. Calibration of the ruby pressure gauge to 800 kbar under quasi-hydrostatic conditions. *J. Geophys. Res.* **1986**, *91*, 4673–4676.

(26) Wang, Y.; Lü, X.; Yang, W.; Wen, T.; Yang, L.; Ren, X.; Wang, L.; Lin, Z.; Zhao, Y. Pressure-induced phase transformation, reversible amorphization, and anomalous visible light response in organolead bromide perovskite. *J. Am. Chem. Soc.* **2015**, *137*, 11144–11149.

(27) Kresse, G.; Furthmüller, J. Efficient iterative schemes for *ab initio* total-energy calculations using a plane-wave basis set. *Phys. Rev. B: Condens. Matter Mater. Phys.* **1996**, *54*, 11169–11186.

(28) Perdew, J. P.; Burke, K.; Ernzerhof, M. Generalized gradient approximation made simple. *Phys. Rev. Lett.* **1996**, *77*, 3865–3868.

(29) Prescher, C.; Prakapenka, V. B. DIOPTAS: a program for reduction of two-dimensional X-ray diffraction data and data exploration. *High Pressure Res.* **2015**, *35*, 223–230.

(30) Rodríguez-Carvajal, J. Recent advances in magnetic structure determination by neutron powder diffraction. *Phys. B* **1993**, *192*, 55–69.

(31) Vankó, G.; Neisius, T.; Molnár, G.; Renz, F.; Kárpáti, S.; Shukla, A.; de Groot, F. M. F. Probing the 3d spin momentum with X-ray emission spectroscopy: The case of molecular-spin transitions. *J. Phys. Chem. B* **2006**, *110*, 11647–11653.

(32) Donnay, G.; Corliss, L. M.; Donnay, J. D. H.; Elliott, N.; Hastings, J. M. Symmetry of magnetic structures: magnetic structure of chalcopyrite. *Phys. Rev.* **1958**, *112*, 1917–1923.

(33) Boekema, C.; Krupski, A. M.; Varasteh, M.; Parvin, K.; Van Til, F.; Van Der Woude, F.; Sawatzky, G. A. Cu and Fe valence states in CuFeS₂. *J. Magn. Magn. Mater.* **2004**, *272-276*, 559–561.

(34) Conejeros, S.; Alemany, P.; Lluell, M.; Moreira, I. P. R.; Sánchez, V.; Llanos, J. Electronic structure and magnetic properties of CuFeS₂. *Inorg. Chem.* **2015**, *54*, 4840–4849.

(35) Knight, K. S.; Marshall, W. G.; Zochowski, S. W. The low-temperature and high-pressure thermoelastic and structural properties of chalcopyrite, CuFeS₂. *Can. Mineral.* **2011**, *49*, 1015–1034.

(36) Sainctavit, Ph.; Petiau, J.; Flank, A. M.; Ringeissen, J.; Lewonczuk, S. XANES in chalcopyrites semiconductors: CuFeS₂, CuGaS₂, CuInSe₂. *Phys. B* **1989**, *158*, 623–624.

(37) Pitt, G. D.; Vyas, M. K. R. Metal-semiconductor transition in single crystal chalcopyrite (CuFeS₂). *Solid State Commun.* **1974**, *15*, 899–902.

(38) Tinoco, T.; Itié, J. P.; Polian, A.; San Miguel, A.; Moya, E.; Grima, P.; Gonzalez, J.; Gonzalez, F. Combined x-ray absorption and x-ray diffraction studies of CuGaS₂, CuGaSe₂, CuFeS₂ and CuFeSe₂ under high pressure. *J. Phys. IV* **1994**, *4*, C9-151–C9-154.

(39) Sato, K.; Takahashi, H.; Mori, N.; Minomura, S. Optically detected insulator-metal transition in CuFeS₂. *Prog. Cryst. Growth Charact.* **1984**, *10*, 125–132.

(40) Kobayashi, H.; Umemura, J.; Kazekami, Y.; Sakai, N.; Alfè, D.; Ohishi, Y.; Yoda, Y. Pressure-induced amorphization of CuFeS₂ studied by ⁵⁷Fe nuclear resonant inelastic scattering. *Phys. Rev. B: Condens. Matter Mater. Phys.* **2007**, *76*, 134108.

(41) Rueff, J.-P.; Kao, C.-C.; Struzhkin, V. V.; Badro, J.; Shu, J.; Hemley, R. J.; Mao, H. K. Pressure-induced high-spin to low-spin transition in FeS evidenced by X-ray emission spectroscopy. *Phys. Rev. Lett.* **1999**, *82*, 3284–3287.

(42) Lee, M.; Rosenbaum, T. F.; Saboungi, M.-L.; Schnyders, H. S. Band-gap tuning and linear magnetoresistance in the silver chalcogenides. *Phys. Rev. Lett.* **2002**, *88*, 066602.

(43) Xu, W. M.; Rozenberg, G. Kh.; Pasternak, M. P.; Kertzer, M.; Kurnosov, A.; Dubrovinsky, L. S.; Pascarelli, S.; Munoz, M.; Vaccari, M.; Hanfland, M.; Jeanloz, R. Pressure-induced Fe-Cu cationic valence exchange and its structural consequences: High-pressure studies of delafossite CuFeO₂. *Phys. Rev. B: Condens. Matter Mater. Phys.* **2010**, *81*, 104110.